Ecotoxicology and Environmental Safety 88 (2013) 163–168

Contents lists available at SciVerse ScienceDirect

Ecotoxicology and Environmental Safety

journal homepage: www.elsevier.com/locate/ecoenv

# Simultaneous analysis of photosystem responses of *Microcystis aeruginoga* under chromium stress

Shuzhi Wang [a,c], Fulong Chen [a,c], Shuyong Mu [a], Daoyong Zhang [b,**], Xiangliang Pan [a,*], Duu-Jung Lee [a,d]

[a] State Key Laboratory of Desert and Oasis Ecology, Xinjiang Institute of Ecology and Geography, Chinese Academy of Sciences, Urumqi 830011, China
[b] State Key Laboratory of Environmental Geochemistry, Institute of Geochemistry, Chinese Academy of Sciences, Guiyang 550002, China
[c] University of Chinese Academy of Sciences, Beijing 100049, China
[d] Department of Chemical Engineering, National Taiwan University, Taipei 10617, Taiwan

ARTICLE INFO

*Article history:*
Received 19 September 2012
Received in revised form
9 November 2012
Accepted 9 November 2012
Available online 8 December 2012

*Keywords:*
Heavy metals
Cyclic electron flow
Electron transport rate
Freshwater algae
Photosystem I
Photosystem II

ABSTRACT

Chromium (Cr) is a toxic metal that poses a great threat to aquatic ecosystems. Information is limited on coinstantaneous responses of photosystems I (PSI) and II (PSII) to Cr(VI) stress due to lack of instruments that can simultaneously measure PSI and PSII activities. In the present study, responses of quantum yields of energy conversion and electron transport rates of PSI and PSII in *Microcystis aeruginosa* cells to Cr(VI) stress were simultaneously analyzed by a DUAL-PAM-100 system. Quantum yield of cyclic electron flow (CEF) under Cr(VI) stress and its physiological role in alleviating toxicity of Cr(VI) were also analyzed. At 5 mg $L^{-1}$ Cr(VI), quantum yield and electron transport rate of PSII decreased significantly, and light-induced non-photochemical fluorescence quenching lost. Cr(VI) also inhibited efficiency of PSII to use energy under high light more than of PSI. PSII showed lower maximal electron transport rate and light adaptability than PSI. Electron transport rate of PSI was higher and decreased less than that of PSII, implying less sensitivity of PSI to high light and Cr(VI). Energy dissipation through non-light-induced non-photochemical fluorescence quenching increased with increasing Cr(VI) concentration. CEF was stimulated under Cr(VI) treatment and made a significant contribution to quantum yield and electron transport of PSI, which was essential for protection of PSI from stresses of Cr(VI) and high light.



## 1. Introduction

Chromium (Cr) caused widespread environmental problem since its compounds are widely used in various industrial processes such as leather tanning and textile (Yu and Gu, 2008). Cr occurs mainly as trivalent Cr(III) and hexavalent Cr(VI) species, and the toxicity of Cr depends on its species (Pan et al., 2009; Vignati et al., 2010).

Microalgae and cyanobacteria as important primary producers live widely in water bodies. They are also frequently used in environmental risk assessment due to their sensitivity to contaminants (Ma et al., 2004; Pan et al., 2008; Qian et al., 2009). Because Cr is a major pollutant in water bodies, phytoplankton species such as cyanobacteria are frequently exposed to Cr (Appenroth et al., 2001; Mishra and Doble, 2008). Physiological responses of microalgae and cyanobacteria to Cr stress have been investigated extensively. Photosynthetic apparatus is one of the sensitive target sites to Cr toxicity. Cr(VI) is known to inhibit the photosynthesis of various phytoplankton species (Ait Ali et al., 2008; Perreault et al., 2009; Prasad et al., 1991) primarily targeting photosystem II (PSII) (Pan et al., 2009). The inhibitory effects of Cr(VI) were suggested to be located on D1 and oxygen evolving complex, oxidizing and reducing sides of PSII (Ait Ali et al., 2006; Perreault et al., 2009), electron carriers for electron transport between $Q_A$ and $Q_B$ (Appenroth et al., 2001; Pan et al., 2009), and PSII reaction centers (Pan et al., 2009).

Although there are quite a lot of studies on effects of heavy metals on PSII (Pan et al., 2009; Wang and Pan, 2012; Zhang et al., 2010), limited studies reported responses of photosystem I (PSI) to heavy metal treatment. Some researchers found that Cd inhibited PSI activity in *Microcystis* sp. (Neelam and Rai, 2003). On the contrary, Zhou et al. (2006) reported that Cd increased the PSI activity of *M. aeruginosa*.

In most cases, effects of heavy metals on PSII or PSI were studied separately. This means that sometimes such results might not reliably reflect status of PSII or PSI due to close relationship between them. Simultaneous measurements of PSI and PSII activities under stress of heavy metals are needed in order to get more accurate information about effects of heavy metals on photosynthetic apparatus.

* Correspondence to: Laboratory of Environmental Pollution and Bioremediation, State Key Laboratory of Desert and Oasis Ecology, Xinjiang Institute of Ecology and Geography, Chinese Academy of Sciences, Urumqi 830 011, PR China. Fax: +86 991 7885446.
** Corresponding author at: State Key Laboratory of Environmental Geochemistry, Institute of Geochemistry, Chinese Academy of Sciences, Guiyang 550002, China.
*E-mail addresses:* xiangliangpan@163.com, panxl@ms.xjb.ac.cn (X. Pan).

0147-6513/$ - see front matter © 2012 Elsevier Inc. All rights reserved.
http://dx.doi.org/10.1016/j.ecoenv.2012.11.009

Perreault et al. (2009) investigated the toxic effects of dichromate on energy dissipation of PSII and PSI in *Chlamydomonas reinhardtii*, and found that both quantum yield of PSII and PSI were highly decreased under Cr(VI) stress. Cr(VI) strongly increased non-photochemical energy dissipation processes of PSII and PSI in *C. reinhardtii*. However, to date effects of Cr(VI) on PSII and PSI in cyanobacteria and responses of photosynthetic activities such as electron transport in PSII and PSI to Cr(VI) and increasing illumination are unclear. In addition, recent studies showed that cyclic electron flow (CEF) around PSI was stimulated and suggested to be important for photoprotection and photosynthesis under drought and chilling stress (Huang et al., 2010, 2012). Effects of heavy metals on CEF are unknown.

*Microcystis aeruginosa* has often been used as a model microbial species for examining effects of contaminants on photosynthesis (Wang et al., 2012; Zhou et al., 2006). In the present study, *M. aeruginosa* was used to detect the effects of Cr(VI) on PSII and PSI activities with the aid of a Dual-PAM-100 system. The aim of this work was to detect responses of complementary quantum yields of energy conversion in PSI and PSII and CEF of PSI at various concentrations of Cr(VI) and increasing illumination.

## 2. Materials and methods

### 2.1. Culture of Microcystis aeruginosa

*M. aeruginosa* (FACHB-905) was purchased from Freshwater Algae Culture Collection of Institute of Hydrobiology, Chinese Academy of Sciences (Wuhan, China). The stock cultures of *M. aeruginosa* cells were carried out in a BG-11 medium (Stanier et al., 1971) at $24\pm2$ °C under fluorescent white light (30 μmol photons $m^{-2}$ $s^{-1}$, full spectrum lamp, Jinantenghao Scientific Instrument Co., Ltd., China) with a 12:12 h light: dark cycle. Growth of cultures was monitored every day by measuring the absorbance of the cells suspension at 680 nm ($A_{680}$) with a UV2800 spectrophotometer (Unico, Shanghai, China).

### 2.2. Cr(VI) treatments

Cells at exponentially growing phase (initial absorbance $A_{680}$ ~0.8) were harvested for Cr(VI) treatment experiments. The cells were cultured in BG-11 culture medium containing various concentrations of Cr(VI). $K_2Cr_2O_7$ (analytical grade, Tianjin Chemical Reagent Research Institute, China) was applied to achieve the required concentrations of Cr(VI) (0–5 mg $L^{-1}$). The samples without addition of Cr(VI) were used as the control. All treatments and controls were run at the same time. The samples were prepared in a final volume of 25 mL and cultured in 50 mL flasks. All the experimental cultures were incubated under the same culture condition as the stock culture. Measurement of PSII and PSI activities was carried out at 12 h after onset of treatments with various concentrations of Cr(VI).

### 2.3. Measurement of PSI and PSII activities

#### 2.3.1. Application of the Dual-PAM-100 system

A dual-wavelength pulse-amplitude-modulated fluorescence monitoring system (Dual-PAM-100, Heinz Walz GmbH, Germany) was used to simultaneously measure the responses of PSI and PSII activities in *M. aeruginosa* to Cr(VI) (Huang et al., 2010; Suzuki et al., 2011). Measurements were performed using the automated induction program provided by the Dual-PAM software (Pfündel et al., 2008) with a slight modification. PSII and PSI activities were quantified by chlorophyll fluorescence and $P700^+$ absorbance changes.

The cell suspension (2.5 mL), which was cultured in BG-11 medium containing various concentrations of Cr(VI) for 12 h as described above, was injected into the DUAL-K25 quartz glass cuvette. It was then placed between the emitter head and detector head of the system. After the sample was dark adapted for 5 min, saturation pulse method was used to detect the maximum fluorescence and maximal change in $P700^+$ signal. The minimal fluorescence after dark-adaptation ($F_0$) was measured at light at low intensity (measuring beam at 0.2 μmol photons $m^{-2}$ $s^{-1}$). A saturating pulse at an irradiance of 10,000 μmol photons $m^{-2}$ $s^{-1}$ was then applied for 300 ms to detect the maximum fluorescence ($F_m$). P700 redox state was measured with a dual wavelength (830/875 nm) unit and was quantified as the difference between the signals at 875 nm and 830 nm. The maximal change in $P700^+$ signal ($P_m$) was determined through application of a saturation pulse after far-red pre-illumination for 10 s according to the methods of Klughammer and Schreiber (1994, 2008b).

#### 2.3.2. Measurement of the slow induction curve under steady actinic light

After determination of $F_0$, $F_m$ and $P_m$, slow induction curve was recorded with the routine of the Dual-PAM software. The actinic light was applied at 30 μmol $m^{-2}$ $s^{-1}$, which was the same as the light intensity for culturing the cyanobacterial cells. A saturating pulse with duration of 300 ms was applied every 20 s after onset of the actinic light to determine the maximum fluorescence signal ($F_m'$) and maximum $P700^+$ signal ($P_m'$) under the actinic light. $P_m'$ was also defined in analogy to the fluorescence parameter $F_m'$ and determined similarly to $P_m$ but without far-red illumination (Huang et al., 2012). The slow induction curve was recorded for 120 s to achieve the steady state of the photosynthetic apparatus, and then the actinic light was turned off. The data derived after the final saturating pulse was used for analysis of activities of PSI, PSII and CEF based on determined $F_0$, $F_m$ and $P_m$.

#### 2.3.3. Quantum yields of the photosystems and CEF

Quantum yields of PSII and PSI were recorded at steady state under the actinic light. The effective photochemical quantum yield of PSII, [$Y$(II)], the quantum yield of light-induced non-photochemical fluorescence quenching, [$Y$(NPQ)], and the quantum yield of non-light-induced non-photochemical fluorescence quenching, [$Y$(NO)], were calculated by the Dual-PAM software (Kramer et al. 2004) and were transformed into the following simpler equations (Klughammer and Schreiber, 2008a; Suzuki et al., 2011):

$$Y(\mathrm{II})=(F_m'-F)/F_m', \quad Y(\mathrm{NPQ})=F/F_m'-F/F_m' \quad \text{and} \quad Y(\mathrm{NO})=F/F_m.$$

where $F$ was the steady-state fluorescence; $F$ and $F_m'$ were detected at the final saturating pulse during the process of slow induction curve.

The effective photochemical quantum yield of PSI, [$Y$(I)], the quantum yield of non-photochemical energy dissipation in PSI due to donor side limitation, [$Y$(ND)], and the quantum yield of non-photochemical energy dissipation in PSI due to acceptor side limitation, [$Y$(NA)], were calculated according to Klughammer and Schreiber (2008b) and Suzuki et al. (2011) as mentioned below:

$$Y(I)=(P_m'-P)/P_m, \quad Y(\mathrm{ND})=(P-P_0)/P_m, \quad Y(\mathrm{NA})=(P_m-P_m')/P_m$$

where $P$ was the $P700^+$ signal recorded just before a saturation pulse. Then a saturation pulse was applied to determine maximum $P700^+$ signal ($P_m'$). Finally at the end of the 1 s dark interval following each saturation pulse, $P_0$ was detected. The signals $P$ and $P_m'$ were detected referencing against $P_0$ (Pfündel et al., 2008). The quantum yield of CEF was calculated from the difference between $Y$(I) and $Y$(II) (Huang et al., 2010):

$$Y(\mathrm{CEF})=Y(I)-Y(\mathrm{II})$$

#### 2.3.4. Electron transport rates in PSI and PSII

Electron transport rates (ETRs) in PSI [ETR(I)] and PSII [ETR(II)] were recorded during the measurement of the slow induction curve and calculated by the Dual-PAM software as follows (Maxwell and Johnson, 2000; Suzuki et al., 2011):

$$\mathrm{ETR}(I)=Y(I)\times \mathrm{PAR}\times 0.84\times 0.5$$

$$\mathrm{ETR}(\mathrm{II})=Y(\mathrm{II})\times \mathrm{PAR}\times 0.84\times 0.5$$

#### 2.3.5. Relation between cyclic electron flow (CEF) and linear electron flow (LEF)

CEF and LEF were detected by calculating the changes of the ratios of $Y$(CEF)/$Y$(I), $Y$(CEF)/$Y$(II) and $Y$(II)/$Y$(I) after onset of various treatments for 12 h. $Y$(CEF)/$Y$(I), $Y$(II)/$Y$(I) and $Y$(CEF)/$Y$(II) indicated the contribution of CEF to $Y$(I), the contribution of LEF to $Y$(I), and the relation between the quantum yield of CEF and LEF, respectively. The ratio of $Y$(II)/$Y$(I) also showed the distribution of quantum yield between two photosystems (Huang et al., 2010).

#### 2.3.6. Measurement of rapid light response curves of ETR(I) and ETR(II)

After the record for slow induction curve, the rapid light curves (RLCs) of ETR(I) and ETR(II) were recorded in the rapid light curve mode (RLC mode) with the routine of the Dual-PAM software to detect the response of the activities of electron transport in PSI and PSII to increasing illumination under exposure to Cr(VI). After the RLC mode was turned on, the actinic light was applied for 30 s to each of a series of increasing intensity (0–1311 μmol photons $m^{-2}$ $s^{-1}$). A saturating pulse was applied after each period of actinic light to determine $F_m'$ and $P_m'$. RLCs with saturation pulse analysis were based on determined $F_0$, $F_m$ and $P_m$.

ETR(I) and ETR(II) were defined and calculated using the Dual-PAM software as described above. Descriptive parameters of ETR(I) and ETR(II) during the light response reaction, the initial slope of RLC of ETR(I) or ETR(II) ($\alpha$), the maximal electron transport rates in PSI or PSII ($ETR_{max}$) and the index of light adaptation of PSI or PSII ($I_k$, $ETR_{max}/\alpha$) were derived from the RLCs, which were automatically calculated by the Dual-PAM software according to the exponential function described by Platt et al. (1980) and Kühl et al. (2001).

### 2.4. Statistics

Each treatment was replicated four times. Means and standard deviation (S.D.) were calculated for each treatment from four replicate samples and have been

presented in tables and figures. Student's *t*-test and Analysis of Variance (one-way ANOVA) were performed to detect the significance of differences between treatments and control. The post-hoc least significant difference (LSD) test was used to establish significant differences among the treatments. Statistical significance was accepted when *P* value was less than 0.05.

## 3. Results

### 3.1. Effects of Cr(VI) on quantum yields of energy conversion in PSI and PSII

Complementary quantum yields of energy conversion in PSI and PSII of *M. aeruginosa* were detected at steady state from the slow induction curve after exposure to various concentrations of Cr(VI) for 12 h (Table 1). After exposure to 0.5 mg $L^{-1}$ Cr(VI), the parameters of the complementary quantum yields of energy conversion in PSI and PSII did not show significant difference from that of control. *Y*(II) decreased with increasing Cr(VI) concentration and were significantly lower when the cells were treated at $\geq$ 1.0 mg $L^{-1}$ of Cr(VI) whereas *Y*(ND) showed a minor but significant increase at 5 mg $L^{-1}$ of the metal. *Y*(I) significantly decreased at 5 mg $L^{-1}$ Cr(VI) compared to the control. Y(NA) was not significantly changed with Cr(VI) treatment. *Y*(NO) and *Y*(NPQ) showed no significant change at $\leq$ 1.0 mg $L^{-1}$ of Cr(VI). *Y*(NO) significantly increased, but *Y*(NPQ) dropped to zero at 5 mg $L^{-1}$ (Table 1).

### 3.2. Effects of Cr(VI) on CEF around PSI

The value of *Y*(CEF) increased with increasing Cr(VI) concentration, indicating the activation of CEF on exposure to Cr(VI). Significant increase of *Y*(CEF), compared to control, was however observed only at 5 mg $L^{-1}$ of Cr(VI) after 12 h of treatment ($P < 0.05$; *t*-test) (Fig. 1).

The ratios of *Y*(CEF)/*Y*(I) and *Y*(CEF)/*Y*(II) increased with increasing Cr(VI) concentration, where the ratio of *Y*(CEF)/*Y*(II) increased from 2.1 in the control to 6.0 in the treatment with 5 mg $L^{-1}$ Cr(VI) (285% increase, compared to control). The ratio of *Y*(II)/*Y*(I), on the other hand, significantly decreased with increasing concentration of Cr(VI) (Fig. 2).

### 3.3. Responses of electron transport rates in PSI and PSII

ETR(I) and ETR(II) decreased with increasing Cr(VI) concentration and ETR(II) was lower than ETR(I) in *M. aeruginosa*. There was a continuous concentration-dependent decrease of ETR in both PS and significant reduction was noted when cells were treated with $\geq$ 1.0 mg $L^{-1}$ of Cr(VI) (Fig. 3). Comparison between two PS showed that the rate of reduction of ETR was more in PSII than in PSI, indicating greater adverse effect on PSII than on PSI ($P < 0.05$; one-way ANOVA, post-hoc test LSD).

### 3.4. Effects of Cr(VI) on the RLCs of ETR(I) and ETR(II)

The RLCs of ETR(I) (Fig. 4A) and ETR(II) (Fig. 4B) decreased with increasing concentration of Cr(VI) after 12 h of treatment. The change in amplitudes of the RLCs of ETR(I) were higher than that of ETR(II). The amplitude of the whole RLCs of ETR(I) slightly decreased with increasing concentration of Cr(VI) and only showed significant decrease at 5 mg $L^{-1}$. ETR(I) increased with increasing light intensity up to 555 μmol photons $m^{-2}$ $s^{-1}$, and showed little or no decrease at all other higher illuminations. The RLCs of ETR(II) showed no significant difference between treatment with 0.5 mg $L^{-1}$ Cr(VI) and the control, whereas at all other higher concentrations these were significantly lowered than that of control. The RLCs of ETR(II) drastically decreased and lost the shape when the cells were treated with 5 mg $L^{-1}$ Cr(VI). The RLCs of ETR(II) increased with the increase of light intensity up to 240 μmol photons $m^{-2}$ $s^{-1}$ after exposure to 5 mg $L^{-1}$ Cr(VI) for 12 h, but a continuous decrease was observed thereafter. In control and at treatment with $\leq$ 1.0 mg $L^{-1}$ of Cr(VI) the amplitude of RLCs of ETR(II) increased up to 363 μmol photons $m^{-2}$ $s^{-1}$ and decreased steadily thereafter. On comparison of the rate of increase, however, with increase of irradiance, it was observed that the rate of change of RLCs of ETR(II) decreased with the increase of metal concentration ($\leq$ 1.0 mg $L^{-1}$).

More information about the RLCs of ETR(I) and ETR(II) could be derived from the descriptive parameters (Table 2). $I_k$ of the RLCs of ETR(I) did not show significant difference between different treatments and control. Whereas $\alpha$ and $ETR_{max}$ of the RLCs of ETR(I) decreased with increasing Cr(VI) concentration and significantly decreased at 5 mg $L^{-1}$ ($P < 0.05$). $I_k$, $\alpha$ and $ETR_{max}$ of the RLCs of ETR(II) were lower than those of ETR(I) in different treatments, and decreased with increasing Cr(VI) concentration. $I_k$ of the RLCs of ETR(II) significantly decreased when the cells were treated with 5 mg $L^{-1}$ Cr(VI), and $\alpha$ and $ETR_{max}$ showed significant decrease for treatments with $\geq$ 1 mg $L^{-1}$ Cr(VI) (Table 2).

## 4. Discussion

Toxic effects of Cr(VI) on PSI and PSII activities of *M. aeruginosa* were examined simultaneously in the present study. The quantum yields of PSI, PSII and CEF were analyzed to detect the responses of PSI and PSII to Cr(VI) treatment, and to detect whether CEF was enhanced under Cr(VI) stress. The RLCs of ETR(I) and ETR(II) during light response reaction were also measured to show the responses of the activities of PSI and PSII to increasing illumination during exposure to Cr(VI).

**Table 1**
The complementary quantum yields of energy conversion in PSI and PSII of *M. aeruginosa* after exposure to various concentrations of Cr(VI) for 12 h. Data were detected by saturating pulse during the process of slow induction curve. The actinic light was supplied at the intensity of 30 μmol $m^{-2}$ $s^{-1}$ for 120 s to measure the slow induction curve.

| Cr(VI) | Quantum yields in PSI | | | Quantum yields in PSII | | |
|---|---|---|---|---|---|---|
| (mg $L^{-1}$) | *Y*(I) | *Y*(ND) | *Y*(NA) | *Y*(II) | *Y*(NO) | *Y*(NPQ) |
| 0 | 0.88 ± 0.01 | 0.00 ± 0.01 | 0.12 ± 0.01 | 0.28 ± 0.01 | 0.68 ± 0.05 | 0.04 ± 0.03 |
| 0.5 | 0.86 ± 0.04 | 0.00 ± 0.01 | 0.13 ± 0.05 | 0.26 ± 0.04 | 0.71 ± 0.05 | 0.03 ± 0.03 |
| 1 | 0.83 ± 0.03 | 0.01 ± 0.01 | 0.17 ± 0.03 | 0.22 ± 0.02* | 0.74 ± 0.03 | 0.04 ± 0.03 |
| 5 | 0.79 ± 0.07* | 0.09 ± 0.05* | 0.13 ± 0.06 | 0.10 ± 0.04* | 0.90 ± 0.04* | 0.00 ± 0.00* |

* Significant at $P < 0.05$ (one-way ANOVA, post-hoc test LSD); *Y*(I), the effective photochemical quantum yield of PSI; *Y*(ND), the quantum yield of non-photochemical energy dissipation in PSI due to donor side limitation; *Y*(NA), the quantum yield of non-photochemical energy dissipation in PSI due to acceptor side limitation; *Y*(II), the effective photochemical quantum yield of PSII; Y(NO), the quantum yield of non-light-induced non-photochemical fluorescence quenching; *Y*(NPQ), the quantum yield of light-induced non-photochemical fluorescence quenching.

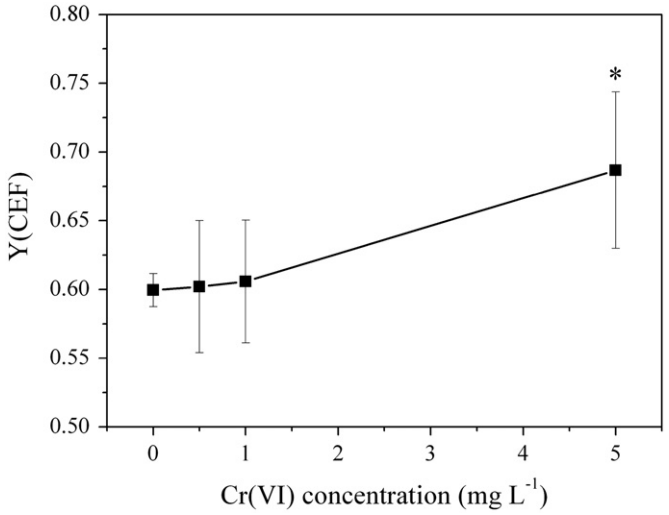


**Fig. 1.** Quantum yield of cyclic electron flow (CEF) [*Y*(CEF)] in *Microcystis aeruginosa* after exposure to various concentrations of Cr(VI) for 12 h. Data were detected at steady state from the slow induction curve by applying light at 30 μmol photons $m^{-2}$ $s^{-1}$ for 120 s. Asterisk indicates that the mean value of *Y*(CEF) for 5 mg $L^{-1}$ Cr(VI) treatment was significantly different from the control ($P < 0.05$; *t*-test).

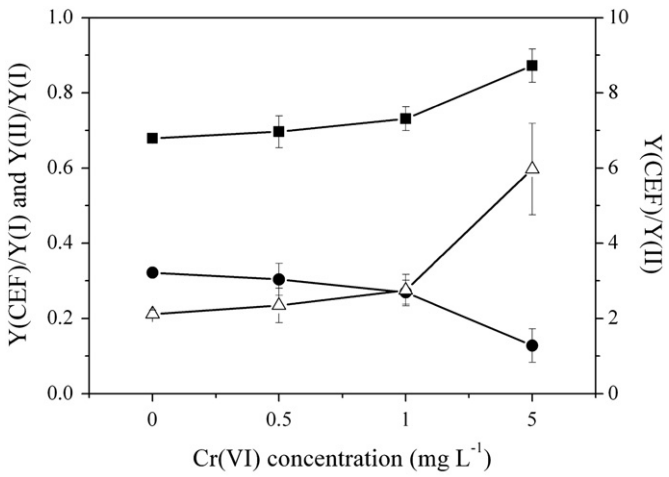


**Fig. 2.** Changes of the ratios of *Y*(CEF)/*Y*(I) (closed square), Y(CEF)/Y(II) (open triangle) and *Y*(II)/*Y*(I) (closed circle) of *M. aeruginosa*. These ratios were calculated from the value of *Y*(I), *Y*(II) and *Y*(CEF) measured at steady state from the slow induction curve after exposure to various concentrations of Cr(VI) for 12 h. *Y*(I), the effective photochemical quantum yield of PSI; *Y*(II), the effective photochemical quantum yield of PSII; *Y*(CEF), the quantum yield of cyclic electron flow.

Some studies reported that Cr(VI) inhibited a variety of metabolic activities (Bishnoi et al., 1993), and photosynthetic apparatus was an important targeted site for its toxicity (Appenroth et al., 2001). Perreault et al. (2009) found that Cr(VI) had different sites of inhibition, associating with PSII, PSI and electron transport sink beyond photosystems. In the present study, after exposure to various concentration of Cr(VI), *Y*(II) showed more significant decrease than that of *Y*(I) in *M. aeruginosa* (Table 1). PSII was more susceptible to Cr(VI) treatment than PSI. This was in agreement with some previous studies that PSII was a main target of heavy metals or other environmental stressors (Mohapatra et al., 2010; Pan et al., 2009, 2011).

Some studies investigated the effects of heavy metals on photosystem I (PSI) and suggested that PSI was less sensitive to heavy

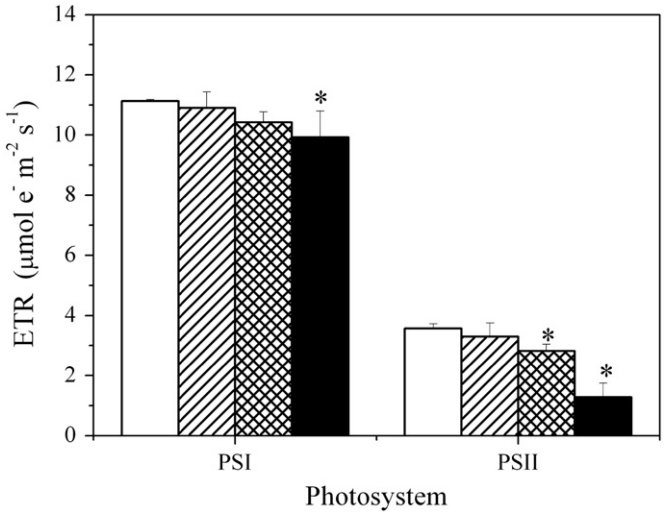


**Fig. 3.** ETR(I) and ETR(II) of *M. aeruginosa* treated with 0 (white columns), 0.5 (striped columns), 1 (gridded columns) and 5 (black columns) mg $L^{-1}$ Cr(VI) for 12 h. ETR(I) and ETR(II) are the electron transport rates of PSI and PSII, respectively. Asterisks indicate that the mean values are significantly different from the control ($P < 0.05$; One-way ANOVA, post-hoc test LSD).

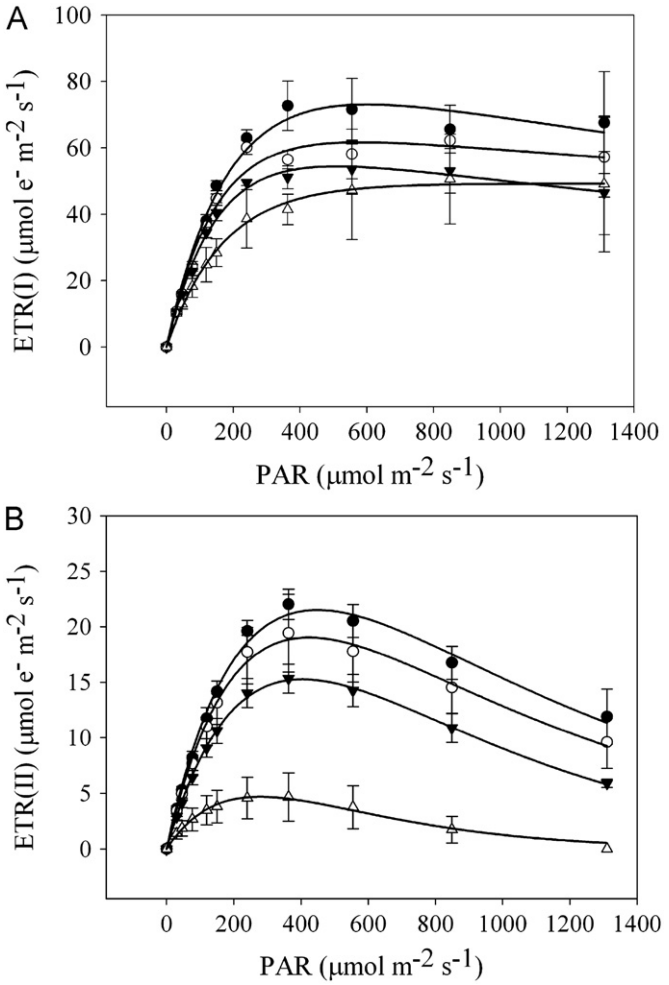


**Fig. 4.** Rapid light curves (RLCs) of (A) ETR(I) and (B) ETR(II). Data were detected through the light response reaction after exposure to 0 (closed circle), 0.5 (open circle), 1 (closed triangle) and 5 (open triangle) mg $L^{-1}$ Cr(VI) for 12 h at 0–1311 μmol photons $m^{-2}$ $s^{-1}$ PAR. The fitting curves were derived from the exponential function described by Platt et al. (1980).

**Table 2**
Descriptive parameters of the light response reaction derived from the rapid light curves (RLCs) of ETR(I) and ETR(II) measured after exposure of *M. aeruginosa* to various concentrations of Cr(VI) for 12 h.

| Cr(VI) | Parameters of RLCs of ETR(I) | | | Parameters of RLCs of ETR(II) | | |
|---|---|---|---|---|---|---|
| ($mg\ L^{-1}$) | $I_k$ ($\mu mol\ photon\ m^{-2}\ s^{-1}$) | $\alpha$ ($e^-\ photon^{-1}$) | $ETR_{max}$ ($\mu mol\ e^-\ m^{-2}\ s^{-1}$) | $I_k$ ($\mu mol\ photon\ m^{-2}\ s^{-1}$) | $\alpha$ ($e^-\ photon^{-1}$) | $ETR_{max}$ ($\mu mol\ e^-\ m^{-2}\ s^{-1}$) |
| 0 | $160.93 \pm 19.44$ | $0.46 \pm 0.02$ | $74.03 \pm 7.48$ | $154.87 \pm 6.30$ | $0.14 \pm 0.01$ | $21.53 \pm 1.08$ |
| 0.5 | $144.98 \pm 41.49$ | $0.45 \pm 0.07$ | $63.43 \pm 6.57$ | $145.75 \pm 6.11$ | $0.13 \pm 0.02$ | $19.03 \pm 3.02$ |
| 1 | $132.10 \pm 27.77$ | $0.43 \pm 0.05$ | $55.20 \pm 4.19$ | $145.55 \pm 5.05$ | $0.11 \pm 0.01$* | $15.25 \pm 1.47$* |
| 5 | $141.40 \pm 2.12$ | $0.28 \pm 0.05$* | $41.70 \pm 10.89$* | $105.90 \pm 2.97$* | $0.05 \pm 0.01$* | $5.67 \pm 0.81$* |

* Significant at $P < 0.05$ (one-way ANOVA, post-hoc test LSD); $\alpha$, the initial slope of RLC of ETR(I) or ETR(II), which reflected the photochemical efficiency (Saroussi and Beer, 2007); $ETR_{max}$, the maximal electron transport rates in PSI or PSII; $I_k$, the index of light adaptation of PSI or PSII, was calculated as $ETR_{max}/\alpha$ (Platt et al., 1980; Kühl et al., 2001).

metals than PSII (Atal et al., 1991; Siedlecka and Krupa, 1996). The less sensitivity of PSI was also observed when the cells were treated with Cr(VI) in the present study, indicated by the less decrease of Y(I) and ETR(I). When the cells were treated with 1 and 5 $mg\ L^{-1}$ Cr(VI), ETR(II) significantly decreased to 36% of the control. However, ETR(I) was still kept at 89% of the control.

*Y*(II) decreased due to the inhibitory effects of heavy metals on different sites of PSII-PSI activity as found in some previous studies (Ait Ali et al., 2006; Perreault et al., 2009). The sites of Cr(VI) with the quantum yield of PSII are suggested to be located on D1 and oxygen evolving complex, i.e., the oxidizing and reducing sides of PSII (Ait Ali et al., 2006; Perreault et al., 2009). Perreault et al. (2009) found that the decrease of *Y*(II) was concomitant with the increase of *Y*(NO) and *Y*(NPQ), mainly due to the increase of *Y*(NO). *Y*(NO) was suggested as a good indicator of PSII damage as shown in other studies (Huang et al., 2010; Perreault et al., 2009; Suzuki et al., 2011). The significant increase of *Y*(NO) was also found when *M. aeruginosa* cells were treated with 5 $mg\ L^{-1}$ Cr(VI), which caused the decrease of *Y*(II). These results indicate that *Y*(NO) is a good indicator of PSII damage under heavy metal stress. After exposure to 5 $mg\ L^{-1}$ Cr(VI) for 12 h, *Y*(NPQ) dropped to zero. The loss of NPQ implies the damage of the energy regulating mechanism of energy conversion in PSII since NPQ is a protective mechanism via carotenoid mediated heat dissipation (Suzuki et al., 2011).

The relation of CEF and LEF after exposure to various concentrations of Cr(VI) could be derived from the change of the ratios of *Y*(CEF)/*Y*(I), *Y*(II)/*Y*(I) and *Y*(CEF)/*Y*(II). Although both *Y*(I) and *Y*(II) decreased with increasing concentration of Cr(VI), the significant decrease of *Y*(II) caused the decrease of the ratio of *Y*(II)/*Y*(I). The decrease of the ratio of *Y*(II)/*Y*(I) with increasing Cr(VI) concentration also showed imbalanced distribution of quantum yield between two photosystems, suggesting that Cr(VI) has more serious inhibition on PSII compared to PSI.

CEF was stimulated due to Cr(VI) treatment as shown by the increase of the value of *Y*(CEF) with increasing Cr(VI) concentration (Fig. 1). The activation of CEF also led to the increase of the ratio of *Y*(CEF)/*Y*(I) (Fig. 2). The ratio of *Y*(CEF)/*Y*(II) increased with increasing Cr(VI) concentration, and the contribution of CEF to quantum yield of PSI was 6 fold of that of LEF when the cells were treated with 5 $mg\ L^{-1}$ Cr(VI). The enhancement of the contribution of CEF to the quantum yield of PSI was important for the less sensitivity of PSI to Cr(VI) treatment. This was also shown by the bigger change of amplitude of the RLCs of ETR(II) and the slight decrease of RLCs of ETR(I) as Cr(VI) concentration increased. CEF made a significant contribution to the quantum yield and the electron transport of PSI under Cr(VI) stress, and the stimulation of CEF was essential for the protection of PSI under stress of Cr(VI) and other stresses (Gao and Wang, 2012; Huang et al., 2010).

The electron transport rate in PSII was more susceptible to high light and Cr(VI). The RLCs of ETR(II) obviously began to decrease at a light intensity lower than that of ETR(I). The RLCs of ETR(II) drastically decreased and lost the shape when the cells were treated with 5 $mg\ L^{-1}$ Cr(VI) for 12 h. The ability of light adaptation and maximal ETR of PSII were lower than those of PSI, indicated $I_k$ and $ETR_{max}$ (Table 2). The decrease of $I_k$, $\alpha$ and $ETR_{max}$ of ETR(II) with increasing Cr(VI) concentration showed that the metal caused more serious inhibition of the efficiency of PSII to use light, especially under high illumination. In contrary, the parameters of RLCs of ETR(I) were higher and showed less decrease of such ability of PSI compared to those of ETR(II), indicating less sensitivity of PSI to high light under Cr(VI) stress (Table 2).

## 5. Conclusions

In the present study, responses of PSII and PSI activities of *M. aeruginosa* to Cr(VI) stress were measured simultaneously. In comparison with PSI, PSII was more susceptible to Cr(VI) and excessive illumination. Cr(VI) had more inhibition on PSII compared to PSI, indicated by the significant decrease of quantum yield and electron transport rates in PSII, and the loss of NPQ after exposure to 5 $mg\ L^{-1}$ Cr(VI). The increase of *Y*(NO) under Cr(VI) stress indicated the damage of PSII by chromium treatment. Cr(VI) had more inhibitory effect on the efficiency of PSII to use light energy than of PSI. PSII showed lower maximal ETR and the irradiance at onset of saturation than those of PSI. ETR in PSI was higher and decreased less than those of PSII under Cr(VI) stress, implying less sensitivity of PSI to high light and Cr(VI). Under Cr(VI) stress CEF was enhanced which made a significant contribution to the quantum yield and the electron transport of PSI and was essential for the survival of the cyanobacterium in metal contaminated environment. The measurements of the quantum yields of PSI and PSII were carried out simultaneously with the Dual-PAM-100 system in the present study, which provides more accurate and authentic depiction of the responses of the photosynthetic apparatus. The Dual-PAM-100 system is a powerful tool in ecotoxicity test.

## Acknowledgments

This work was supported by Program of 100 Distinguished Young Scientists of the Chinese Academy of Sciences and National Natural Science Foundation of China (U1120302 and 21177127). We are grateful to the reviewers for their valuable comments that significantly improved our manuscript.

## References


Ait Ali, N., Dewez, D., Didur, O., Popovic, R., 2006. Inhibition of photosystem II photochemistry by Cr is caused by the alteration of both D1 protein and oxygen evolving complex. Photosynth. Res. 89, 81–87.

Ait Ali, N., Juneau, P., Didur, O., Perreault, F., Popovic, R., 2008. Effect of dichromate on photosystem II activity in xanthophyll-deficient mutants of *Chlamydomonas reinhardtii*. Photosynth. Res. 95, 45–53.

Appenroth, K.J., Stöckel, J., Srivastava, A., Strasser, R.J., 2001. Multiple effects of chromate on the photosynthetic apparatus of *Spirodela polyrhiza* as probed by OJIP chlorophyll *a* fluorescence measurements. Environ. Pollut. 115, 49–64.

Atal, N., Saradhi, P.P., Mohanty, P., 1991. Inhibition of the chloroplast photochemical reactions by treatment of wheat seedlings with low concentrations of cadmium: analysis of electron transport activities and changes in fluorescence yield. Plant Cell Physiol. 32, 943–951.

Bishnoi, N.R., Chugh, L.K., Sawhney, S.K., 1993. Effect of chromium on photosynthesis, respiration and nitrogen fixation in Pea (*Pisum sativum* L.) seedlings. J. Plant Physiol. 142, 25–30.

Gao, S., Wang, G., 2012. The enhancement of cyclic electron flow around photosystem I improves the recovery of severely desiccated *Porphyra yezoensis* (Bangiales, Rhodophyta. J. Exp. Bot. 63, 4349–4358.

Huang, W., Yang, S.J., Zhang, S.B., Zhang, J.L., Cao, K.F., 2012. Cyclic electron flow plays an important role in photoprotection for the resurrection plant *Paraboea rufescens* under drought stress. Planta 235, 819–828.

Huang, W., Zhang, S.B., Cao, K.F., 2010. Stimulation of cyclic electron flow during recovery after chilling-induced photoinhibition of PSII. Plant Cell Physiol. 51, 1922–1928.

Klughammer, C., Schreiber, U., 1994. An improved method, using saturating light pulses, for the determination of photosystem I quantum yield via $P700^{+}$-absorbance changes at 830 nm. Planta 192, 261–268.

Klughammer, C., Schreiber, U., 2008a. Complementary PS II quantum yields calculated from simple fluorescence parameters measured by PAM fluorometry and the Saturation Pulse method. PAM Appl. Notes 1, 27–35.

Klughammer, C., Schreiber, U., 2008b. Saturation Pulse method for assessment of energy conversion in PS I. PAM Appl. Notes 1, 11–14.

Kramer, D.M., Johnson, G., Kiirats, O., Edwards, G.E., 2004. New fluorescence parameters for the determination of $Q_A$ redox state and excitation energy fluxes. Photosynth. Res. 79, 209–218.

Kühl, M., Glud, R.N., Borum, J., Roberts, R., Rysgaard, S., 2001. Photosynthetic performance of surface-associated algae below sea ice as measured with a pulse-amplitude-modulated (PAM) fluorometer and $O_2$ microsensors. Mar. Ecol. Prog. Ser. 223, 1–14.

Ma, J.Y., Lin, F.C., Zhang, R.Z., Yu, W.W., Lu, N.H., 2004. Differential sensitivity of two green algae, *Scenedesmus quadricauda* and *Chlorella vulgaris*, to 14 pesticide adjuvants. Ecotoxicol. Environ. Saf. 58, 61–67.

Maxwell, K., Johnson, G.N., 2000. Chlorophyll fluorescence- a practical guide. J. Exp. Bot. 51, 659–668.

Mishra, S., Doble, M., 2008. Novel chromium tolerant microorganisms: isolation, characterization and their biosorption capacity. Ecotoxicol. Environ. Saf. 71, 874–879.

Mohapatra, P.K., Khillar, R., Hansdah, B., Mohanty, R.C., 2010. Photosynthetic and fluorescence responses of *Solanum melangena* L. to field application of dimethoate. Ecotoxicol. Environ. Saf. 73, 78–83.

Neelam, A., Rai, L.C., 2003. Differential responses of three cyanobacteria to UV-B and Cd. J. Microbiol. Biotechnol 13, 544–551.

Pan, X.L., Chen, X., Zhang, D.Y., Wang, J.L., Deng, C.N., Mu, G.J., Zhu, H.S., 2009. Effect of chromium(VI) on photosystem II activity and heterogeneity of *Synechocystis* sp. (cyanophyta): studied with in vivo chlorophyll fluorescence tests. J. Phycol. 45, 386–394.

Pan, X.L., Deng, C.N., Zhang, D.Y., Wang, J.L., Mu, G.J., Chen, Y., 2008. Toxic effects of amoxicillin on the photosystem II of *Synechocystis* sp. characterized by a variety of in vivo chlorophyll fluorescence tests. Aquat. Toxicol. 89, 207–213.

Pan, X.L., Zhang, D.Y., Chen, X., Bao, A.M., Li, L.H., 2011. Antimony accumulation, growth performance, antioxidant defense system and photosynthesis of *Zea mays* in response to antimony pollution in soil. Water Air Soil Pollut. 215, 517–523.

Perreault, F., Ait Ali, N., Saison, C., Popovic, R., Juneau, P., 2009. Dichromate effect on energy dissipation of photosystem II and photosystem I in *Chlamydomonas reinhardtii*. J. Photochem. Photobiol. B 96, 24–29.

Pfündel, E., Klughammer, C., Schreiber, U., 2008. Monitoring the effects of reduced PS II antenna size on quantum yields of photosystems I and II using the Dual-PAM-100 measuring system. PAM Appl. Notes 1, 21–24.

Platt, T., Gallegos, C.L., Harrison, W.G., 1980. Photoinhibition of photosynthesis in natural assemblages of marine phytoplankton. J. Mar. Res. 38, 687–701.

Prasad, S.M., Singh, J.B., Rai, L.C., Kumar, H.D., 1991. Metal-induced inhibition of photosynthetic electron transport chain of the cyanobacterium *Nostoc muscorum*. FEMS Microbiol. Lett. 82, 95–100.

Qian, H.F., Li, J.J., Sun, L.W., Chen, W., Sheng, G.D., Liu, W.P., Fu, Z.W., 2009. Combined effect of copper and cadmium on *Chlorella vulgaris* growth and photosynthesis-related gene transcription. Aquat. Toxicol. 94, 56–61.

Saroussi, S., Beer, S., 2007. Alpha and quantum yield of aquatic plants derived from PAM fluorometry: uses and misuses. Aquat. Bot. 86, 89–92.

Siedlecka, A., Krupa, Z., 1996. Interaction between cadmium and iron and its effects on photosynthetic capacity of primary leaves of *Phaseolus vulgaris*. Plant Physiol. Biochem. 34, 833–841.

Stanier, R., Kunisawa, R., Mandel, M., Cohen-Bazire, G., 1971. Purification and properties of unicellular blue-green algae (order *Chroococcales*). Bacteri ological Rev. 35, 171–205.

Suzuki, K., Ohmori, Y., Ratel, E., 2011. High root temperature blocks both linear and cyclic electron transport in the dark during chilling of the leaves of rice seedlings. Plant Cell Physiol. 52, 1697–1707.

Vignati, D.A.L., Dominik, J., Beye, M.L., Pettine, M., Ferrari, B.J.D., 2010. Chromium(VI) is more toxic than chromium(III) to freshwater algae: a paradigm to revise? Ecotoxicol. Environ. Saf. 73, 743–749.

Wang, S.Z., Pan, X.L., 2012. Effects of Sb(V) on growth and chlorophyll fluorescence of *Microcystis aeruginosa* (FACHB-905). Curr. Microbiol. 65, 733–741.

Wang, S.Z., Zhang, D.Y., Pan, X.L., 2012. Effects of arsenic on growth and photosystem II (PSII) activity of *Microcystis aeruginosa*. Ecotoxicol. Environ. Saf. 84, 104–111.

Yu, X.Z., Gu, J.D., 2008. Effect of available nitrogen on phytoavailability and bioaccumulation of hexavalent and trivalent chromium in hankow willows (*Salix matsudana Koidz*. Ecotoxicol. Environ. Saf. 70, 216–222.

Zhang, D.Y., Pan, X.L., Mu, G.J., Wang, J.L., 2010. Toxic effects of antimony on photosystem II of *Synechocystis* sp. as probed by in vivo chlorophyll fluorescence. J. Appl. Phycol. 22, 479–488.

Zhou, W., Juneau, P., Qiu, B., 2006. Growth and photosynthetic responses of the bloom-forming cyanobacterium *Microcystis aeruginosa* to elevated levels of cadmium. Chemosphere 65, 1738–1746.